Synthesis and characterization of rice husk silica, silica-carbon composite and H_3PO_4 activated silica

(Síntese e caracterização de sílica da palha de arroz, compósito sílica-carbono e sílica ativada por H_3PO_4)

D. Singh, R. Kumar, A. Kumar, K. N. Rai

Materials Science Programme, Materials and Metallurgical Engineering, Chemical Engineering Department
Indian Institute of Technology, Kanpur-208016, India
knrai@iitk.ac.in

Abstract

This paper discusses synthesis and characterization of (i) rice husk based nanosilica, (ii) nanosilica carbon composite granules and (iii) phosphoric acid activated ash silica. These have been produced by burning husk in air, charring husk in hydrogen and activating husk silica with H_3PO_4 respectively. X-ray diffraction studies of these products reveal increasing peak width (amorphosity) with decreasing burning temperature. The activated rice husk silica transforms to crystalline product when burnt above 1000 ℃. The variation of surface area and pore volume with burning temperature show different behavior for air fired and hydrogen charred products. Activation energy associated with change in surface area for air fired and hydrogen charred samples have also been studied. Rate of variation in surface area with temperature indicate different trend. The validations of these products have been evaluated by decolorizing capacity of standard molasses and iodine solution. The adsorptive powers of these products have been found to be highest for activated silica and lowest for hydrogenated ash.

Keywords: rice husk, silica, silica-carbon.

Resumo

A síntese e a caracterização de nanosílica obtida da palha de arroz, compósitos nanosílica-carbono e cinza de sílica ativada com ácido fosfórico são apresentadas. Esses materiais foram produzidos pela queima de palha de arroz ao ar, em hidrogênio e por ativação da cinza da palha de arroz com ácido fosfórico, respectivamente. Análise de difração de raios X destes produtos mostram aumento da largura dos picos (amorfização) com a diminuição da temperatura de queima. A sílica da palha de arroz ativada transforma a produto cristalino quando a temperatura é maior que 1000 °C. A variação da área de superfície específica e do volume de poro com a temperatura de queima mostra comportamento diferente quando a queima é feita ao ar ou sob hidrogênio. A energia de ativação associada com a mudança na área de superfície específica após queima ao ar e sob hidrogênio também foi estudada. A taxa de variação da área de superfície específica com a temperatura mostra diferente tendência. A avaliação dos produtos foi feita por meio da capacidade de descolorimento em soluções de melaço e de iodo. Foi verificado que a capacidade de absorção dos produtos é maior para a sílica ativada e menor para a cinza hidrogenada.

Palavras-chave: palha de arroz, sílica, sílica-carbono.

INTRODUCTION

Ultrafine silica powder and silica/carbon composite find potential applications in many industrially important products. Silica is an important ingredient of high surface area catalyst, sorption media, glass and cement manufacturing and dehydration systems [1]. Similarly high surface area carbon is used in protective mask against war gases, catalysts, odour removal and fillers in rubber industries. Though these products are synthesized using complicated chemical routes [2-4], the rice husk, coming out of rice mills as cheap by product, offer great opportunity for their production at much convenient and reduced expenses. Further more, charring of rice husk produces nanosize silica carbon (called nanosil) intermixed composite which may find newer application

because such product is not available synthetically. This may directly be converted to silicon carbide and silicon nitride at high temperature [5, 6]. The husk ash can also is reduced to much needed silicon, silicon tetrachloride and silane using proper reducing agents [7-10]. In addition, activated white carbon black has been produced [11, 12].

At present, nanoscale silica materials are prepared using several methods, including vapor-phase reaction, sol-gel and thermal decomposition technique. The powder production of silica is a highly energy intensive process. Unlike this, economically viable and high grade nanosize amorphous silica from rice husk can be produced simply by burning under appropriate conditions. The major constituents of rice husk are hydrated silicon and organic materials consisting of cellulose (55-60 wt%, including cellulose and hemicellulose)

and lignin (22 wt.%) [13]. The main advantage of producing silica in this manner is highly reactive nature of silica particle, requiring minimum grinding. The energy for burning is mostly supplied from the carbonaceous part of husk itself. Therefore, attempt by many workers have been made to produce silica from rice husk. Silica having large surface area and high porosity by burning rice husk has been produced [14]. During the process about 20% mass of rice husk remains as ash, this contains 95 wt.% silica. Biogenetic silica has been produced by feeding rice husk in an inclined rotatory furnace at 450 ºC, which was rotated at 1 rpm for 30 min [15]. It was found that leaching of rice husk with HCl at 75 ºC for 1 h prior to combustion produces amorphous silica of complete white color [16]. Silica having purity of 92% and average diameter of 0.04 to 0.05 μm was produced [17]. This production of silica involved four stages: feeding, combustion, spraying and drying. Studies of surface morphology, chemical reactivity and surface area measurements reveal the formation of amorphous silica during ashing. The reactivity was found to be the maximum at ashing temperature range of 400-600 ºC and holding time of 6-12 h. However, it was found to decrease with ashing temperature and hold time [18]. After comparing the X-ray photoelectron spectroscopy peak widths of natural silica with those of rice husk ash, the difference in width has been attributed to variation in immediate chemical environment of silica and oxygen in the husk ash.

Biogenetic silica can be used in industrial waste water treatment [20]. Friction materials having balanced energy absorption coefficient and other friction properties has been prepared by compaction and press sintering (750-850 ºC, 1-10 MPa) of a mixture containing Sn (2-8 wt.%), SiO_2 (2-10 wt.%), rice husk (2-8 wt.%) and rest electrolytic Cu powder [21]. An improved method was used to produce silica with lower sodium content by adding silicate solution to pH 1.5 hydrochloric, citric, or oxalic acid solutions until pH 4.0 was reached [22]. The potential and limits of rice husk to prepare relatively pure activated silica was investigated [23]. For the activated silica, rice husk samples were submitted to a chemical pre-and post-treatment using HCl, H_2SO_4 and NaOH solutions. Samples were incinerated at 600 ºC under static air and flowing atmospheres (air, argon and oxygen). It was observed that active silica with a high specific area could be produced from rice husk ash after heat-treating at 973 K in air [24]. Nano-structured silica powders with high specific surface area were obtained from nonisothermal decomposition of rice husk in an air atmosphere [25].

In the present work an attempt therefore has been made to produce rice husk ash in the atmospheric air and hydrogen followed by extensive investigation using XRD, BET and sintering effects with temperature to understand structural and thermal behavior of these products. As these materials may find immediate use in environmental purification, an attempt has also been made to synthesize activated silica and hydrogen charred nanosils to asses their efficiency in color removal from water caused by organic dyes and iodine solution.

EXPERIMENTAL

Three different categories of ash have been prepared in the present investigation from rice husk. These are atmospheric air burning, charring under hydrogen atmosphere, ash activation by phosphoric acid.

Air burning of rice husk (kept in silica crucible) was carried out at four different temperatures, 400, 600, 750 and 900 ºC followed by furnace cooling. For the production of samples under hydrogen atmosphere, the rice husk samples were kept in a silica crucible and positioned hanging in a vertical heated silica tube heated by resistant heater furnace. When furnace reached the desired temperature, the silica tube containing sample was lowered in the desired heating zone of the furnace after continuous flushing with hydrogen. Hydrogen flow was continued till desired time of 1 h. The silica tube after holding time of 1 h was withdrawn slowly from the furnace and cooled finally in atmosphere to room temperature. TGA of rice husk was taken in air at heating rate of 10 deg/min. As specific surface area of air burnt husk was maximum around 400 ºC, the activation process was adopted for ash powders prepared at 400 ºC. First of all rice husk was burnt in air at 300 ºC for one hour followed by atmospheric cooling to room temperature. Orthophosphoric acid solution (20% in water by volume) was added to the ash in a 250 mL beaker with stirring. The ash kept for sufficient time of about 24 h for the absorption of orthophosphoric acid. Resultant mixture was dried completely by heating (at temperature of 65-70 ºC) followed by keeping in furnace at 300 ºC for 1 h. Small amount of the newly formed ash was taken in a long silica tube and was heated in vacuum for 4 at 5 h different temperatures 600, 700, 800, 900 and 1000 ºC.

The surface area and pore volume of all the samples were determined by BET method using nitrogen adsorption at liquid nitrogen temperature. For this Coulter SA3100tm series surface area and pore size analyzer was used. We have used a Reich Seifert (Germany) Iso Debye Flex X-ray diffractometer machine operating at 30 kV and 20 mA (CuK$_\alpha$ radiation of 1.5418 Å) with scanning speed 3 deg/min in 2θ. Scanning electron microscope (JEOL JSM-840A) was used for microscopic investigation at different magnifications. The powdered samples were mounted on sample holder using graphite paint followed Au-Pd plasma coating to make it conducting. EDAX was employed to investigate the wt.% of silicon, potassium, calcium and iron in husk ash.

Chemical activity was determined by the adsorption capacity of all the three types of the samples having maximum surface area. This was accomplished by their decolorization capacity for standard aqueous solutions of molasses and iodine.

The aqueous solution of molasses were prepared by dissolving 100 g of molasses with 15 g of disodium hydrogen phosphate in 500 mL of distilled water followed by 20% orthophosphoric acid addition in order to adjust the pH of mixture to 6.5. The above solution was further diluted to 1 L. Thus produced standard solution (actually one-tenth of original molasses strength) was assumed to contain 100

units of parent color per 100 mL liquor. A series of solutions were prepared by further diluting 5, 10, and 15 to 60 mL of the above solution to 100 mL of distilled water. The color of these diluted solutions therefore corresponds to 5, 10, 15 to 60% of the original solution. Thus, if 10 mL of standard solution is diluted to 100 mL with distilled water, the color of that mixture would represent a concentration of 10 color units per 100 mL. these solutions were used as reference solutions for comparison of colors. The molasses decolorization was performed on the samples produced (having maximum surface area) by three different methods; ash produced in air at 400 ℃, ash produced in hydrogen atmosphere at 900 ℃, activated husk produced at 800 ℃. For performing molasses test, 0.5 g of the sample was added to 50 mL of standard solution followed by stirring and heating to boil. This was kept for 30 min to allow sufficient time for adsorption. The resulting mixture was filtered through Whatman no. 5 filter paper. The color of the filtrate thus obtained was matched with the reference solutions prepared earlier. The difference in the color units between standard and reference solution gave the percentage of color adsorbed by 0.5 g of sample. The same procedure was repeated with 0.3 and 0.1 g of sample and the percentage of color adsorbed was noted.

Iodine test was performed exactly the same way as molasses test. However, the preparation of standard iodine solution was done by dissolving 4.1 g of potassium iodide and 2.7 g of iodine in 1 L water.

RESULTS AND DISCUSSION

X-ray diffraction pattern of all the samples prepared in air (Fig. 1i) do not show well defined peaks. In all cases, a hump is observed in the 2θ ranging from $16°$ to $39°$, indicating disordered structure. Similarly, X-Ray diffraction pattern of all the samples prepared in hydrogen atmosphere (Fig. 1ii) show a single hump indicating disordered structure. It seems that X-ray diffraction is mainly due to amorphous silica particles. As the atomic scattering factor for carbon is very small, intervening carbon atoms seem to contribute very little with respect to scattering from silica.

The results of X-ray diffraction of the rice husk char (Fig. 2i), produced at 350 °C followed by activation with 20% H_3PO_4 and heating at 600, 700, 800 and 900 °C, again did not show sharp peaks, indicating them to be amorphous. However, samples heated to 1000 °C exhibited, as in Fig.2ii well defined XRD peaks. These have been assigned to calcium silicate ($Ca_7Si_2P_2O_{16}$) formation.

Surface area and pore volume observation of various samples (prepared by air burning, hydrogen charring or phosphoric acid treating) at different temperatures are plotted. The plot between surface area and temperature, as shown in Fig. 3a, indicate decrease in surface area with increasing temperature for air burnt ash. The behavior of porosity with temperature as in Fig. 3b, shows an increasing trend with temperature. This may be due to enhancement of void space by pore collapse with rising temperature. This is also supported by microscopic observation of rice husk ash
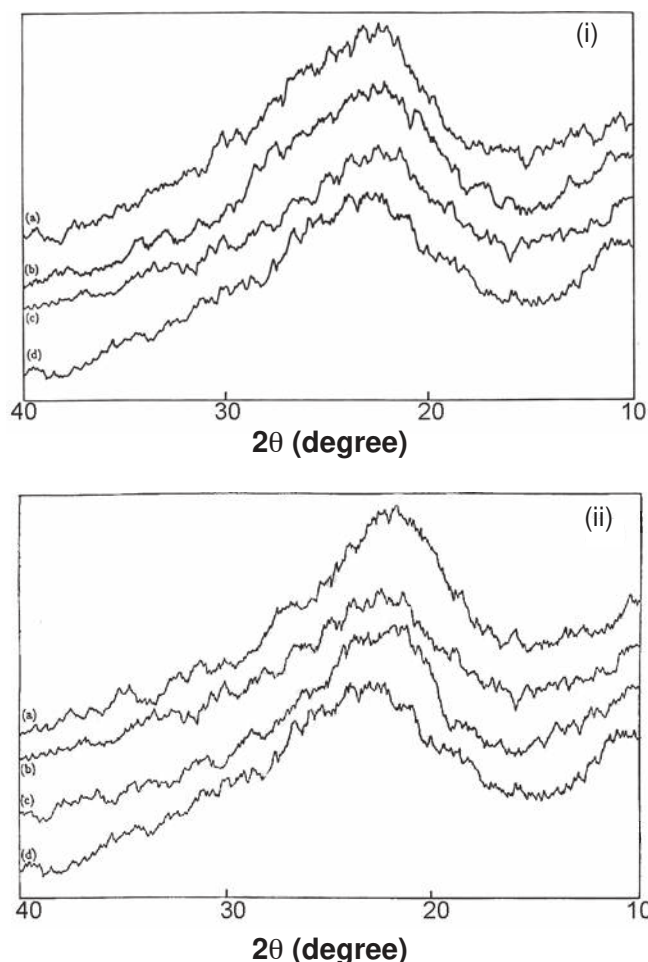

Figure 1: X-Ray diffraction of rice husk ash produced in (i) air and (ii) hydrogen atmosphere at different temperatures (a) 400 °C (b) 600 °C (c) 750 °C and (d) 900 °C.
[Figura 1: Difratogramas de raios X da palha de arroz em (i) ar e (ii) hidrogênio a diferentes temperaturas: (a) 400°C, (b) 600 °C, (c) 750 °C e (d) 900 °C.]

in Fig. 8, showing increasing cavitation in microstructure with increasing temperature.

The surface area and pore volume of all the samples prepared at different temperatures in hydrogen atmosphere are plotted in Fig. 4a. It is evident that the specific surface area increases with charring temperature in this case. The pore volume variation with temperature Fig.4b shows similar trend i.e. it increases with increasing charring temperature. This result is in distinct contrast to rice husk burnt in air, in which surface area decreases and pore volume increases with increasing burning temperature. In the hydrogen charring case, it seems that isolated pores result due to continuously increasing dissociation of hydrocarbon of silica matrix. This leads to increasing number of pores with increasing temperature. Increase in pore volume is therefore natural.

The surface area of air burnt samples of the rice husk ash produced at 350 °C followed by activation with 20% H_3PO_4 and heating at different temperatures are plotted in Fig. 5.
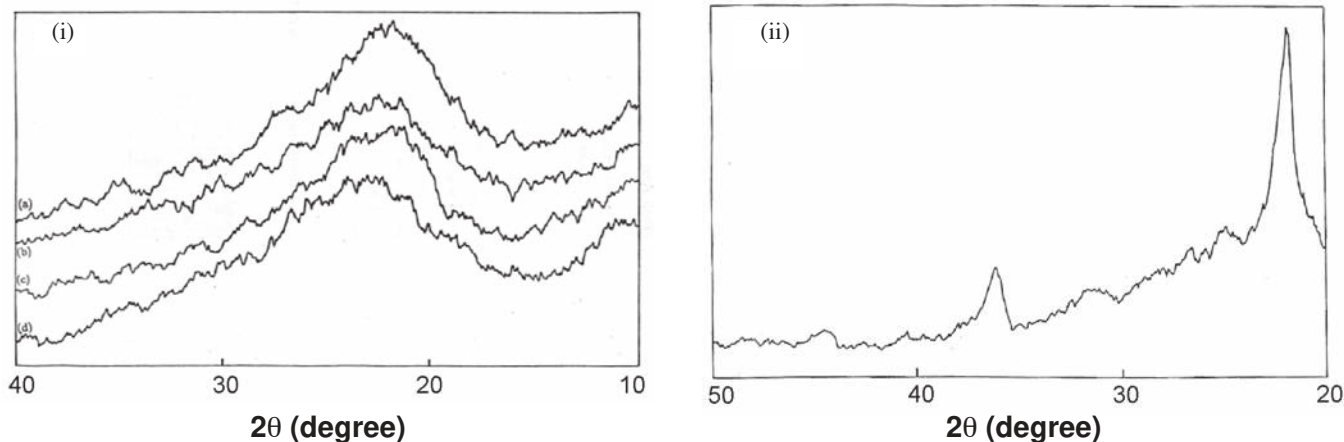
Figure 2: X-ray diffraction pattern of activated husk ash produced at (i) different temperatures: (a) 600 ºC, (b) 700 ºC, (c) 800 ºC and (d) 900 ºC ; and (ii) at 1000 ºC (showing calciumphosphosilicate peaks).
[Figura 2: Difratogramas de raios X da palha de arroz ativada em (i) diferentes temperaturas: (a) 600°C, (b) 700 °C, (c) 800 °C e (d) 900 °C; (ii) a 1000 °C mostrando os picos de silicato de fósforo e cálcio.]
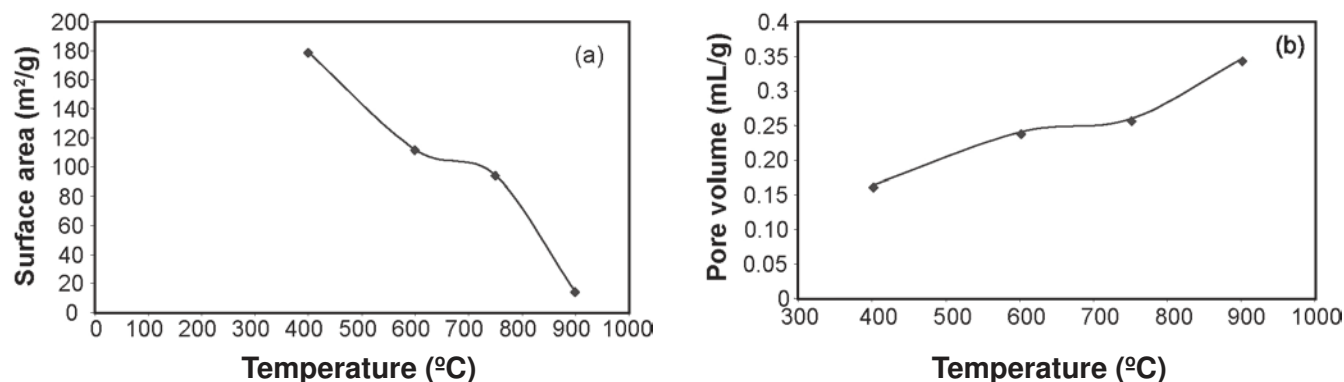

Figure 3: Variation of (a) surface area and (b) pore volume with temperature of air burnt rice husk ash.
[Figura 3: Variação da (a) área de superfície específica e (b) volume de poro da cinza da palha de arroz queimada ao ar.]
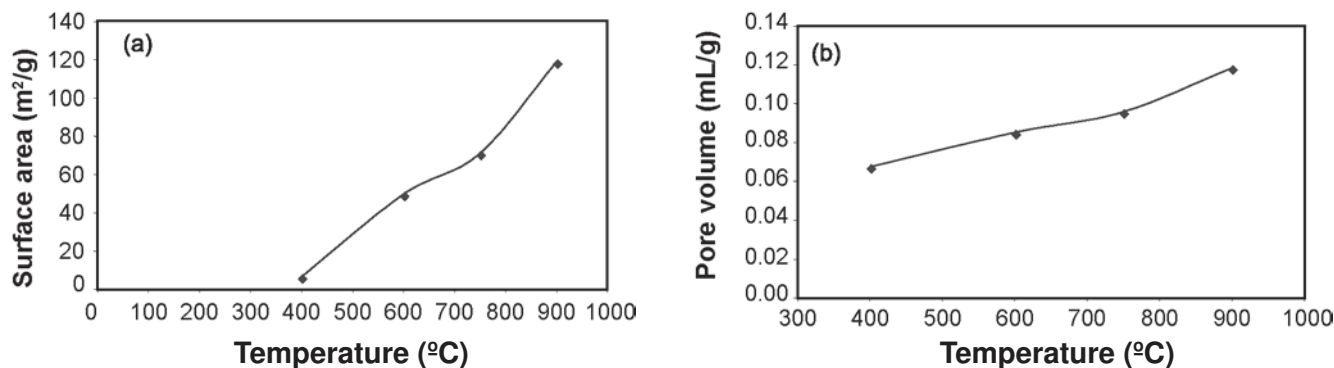
Figure 4: Variation of (a) surface area and (b) pore volume with temperature of hydrogen charred rice husk ash.
[Figura 4: Variação da (a) área de superfície específica e (b) volume de poro da cinza da palha de arroz queimada sob hidrogênio.]

It is interesting to note that surface area (a) first increase from 600 °C onward till around 850 °C and (b) then starts decreasing till 1000 °C. It seems that increase in surface area at lower temperature range (600 to 850 °C) is associated with evaporation of phosphoric acid (H_3PO_4) from pores. However, beyond 850 °C, some kind of solid state reaction starts building up leading to decrease in surface area. This is also suggested by the sharp XRD peak corresponding
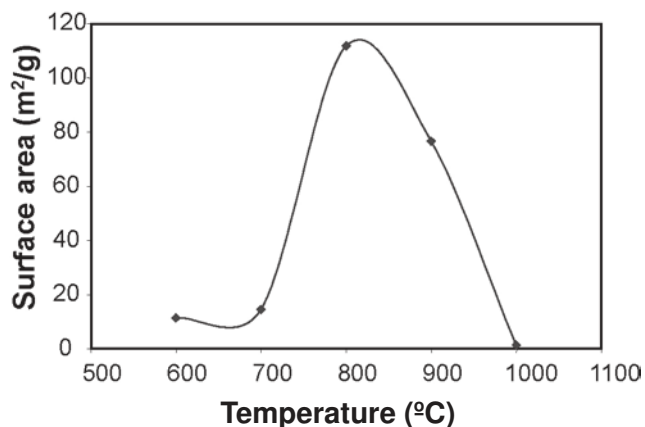
Figure 5: Surface area variation with temperature for activated husk ash.
[Figura 5: Variação da área de superfície específicada cinza da palha de arroz ativada com a temperatura]
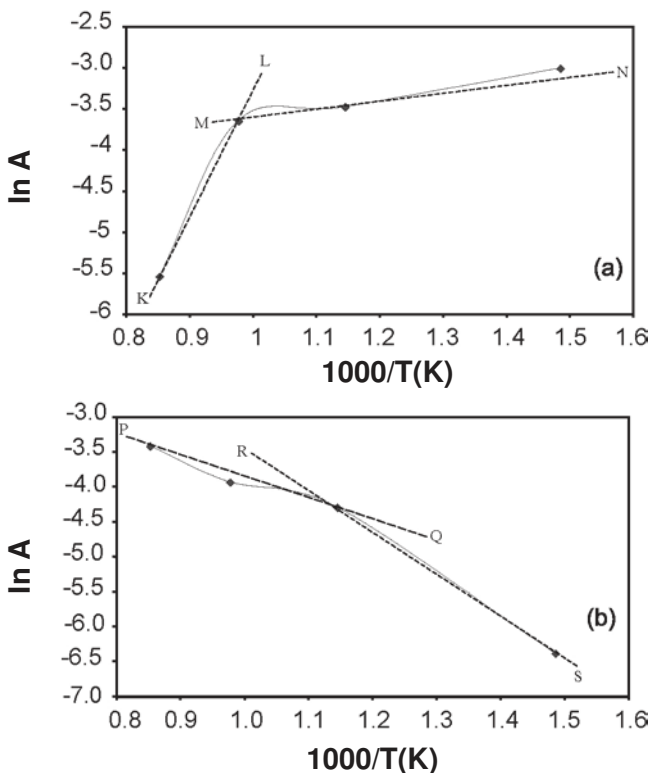

Figure 7: Variation of ln Å with 1/T of activated rice husk ash.
[Figura 7: Variaçao de ln Å com 1/T(K) da cinza da palha de arroz ativada.]

Figure 6: Variation of ln Å with 1/T for rice husk ash produced in (a) air (b) hydrogen atmosphere.
[Figura 6: Variaçao de ln Å com 1/T(K) da cinza da palha de arroz produzida em ar (a) e hidrogênio (b).]

to calcium phospho silicate. Normally samples below 900 °C exhibited XRD pattern with single hump, indicative of amorphous structure.

The activation energy was investigated for the rice husk ash prepared under different conditions. Surface area 'A' of each sample was divided by 3600 s (burning time of 1 h)
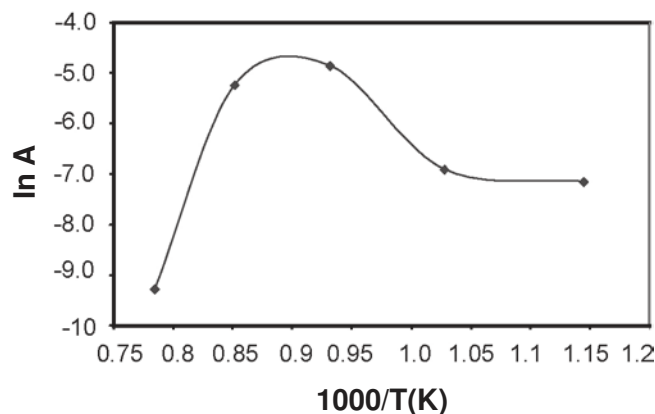
to yield rate of change with time (Å). The variation of ln Å (where Å is equal to A/3600 and A is the surface energy) with 1/T for the rice husk ash, prepared in air at different temperatures, is shown in Fig. 6a. Two different slopes (MN and KL) corresponding to activation energy of 11.47 kJ/mole at lower temperature and 125.77 kJ/mole at higher temperature range is indicative of two distinct processes associated with densification (decreasing surface area) of silica matrix with temperature. Here decreasing ln Å with increasing temperature suggests densification of silica matrix involving bulk and surface diffusion processes. While lower activation energy can be associated with surface diffusion at lower temperature regime, the higher activation energy may be associated with bulk diffusion in amorphous silica matrix. Activation energy for silica has been investigated by both, the theoretical and experimental methods. Based on local density fluctuation concept the diffusion barrier has been assigned values ranging from 1.20 eV (~ 120 kJ/mole) to 2.53 eV (~ 250 kJ/mole) [26]. Experimental method involving diffusion through surface and bulk during oxidation of silicon, barrier values of 1.50 eV to 2.49 eV has been assigned respectively [27]. These values are very close to values observed in the present investigation. In the case of husk ash produced by charring in hydrogen atmosphere, surface area increases continuously with charring temperature. Rate of increase Å in surface area (ln Å) is plotted with 1/T in Fig. 6b.

The lnÅ-1/T plot has changing slope which can approximately be given two distinct slopes, PQ corresponding to activation energy of 25 kJ/mole in high temperature regime and RS with activation energy of 5.1 kJ/mole in low temperature regime. This energy can be associated with barrier for hydrocarbon dissociation and evaporation from silica matrix in which they are intermixed chemically and physically. The change in mechanism takes place around 600 °C. While the process in lower temperature range can be attributed to increasing pore formation due to hydrocarbon evaporation and in high temperature range can be due to pore formation by hydrocarbons dissociation. Plot in Fig.7, between lnÅ and 1/T for air burnt, H_3PO_4 activated ash
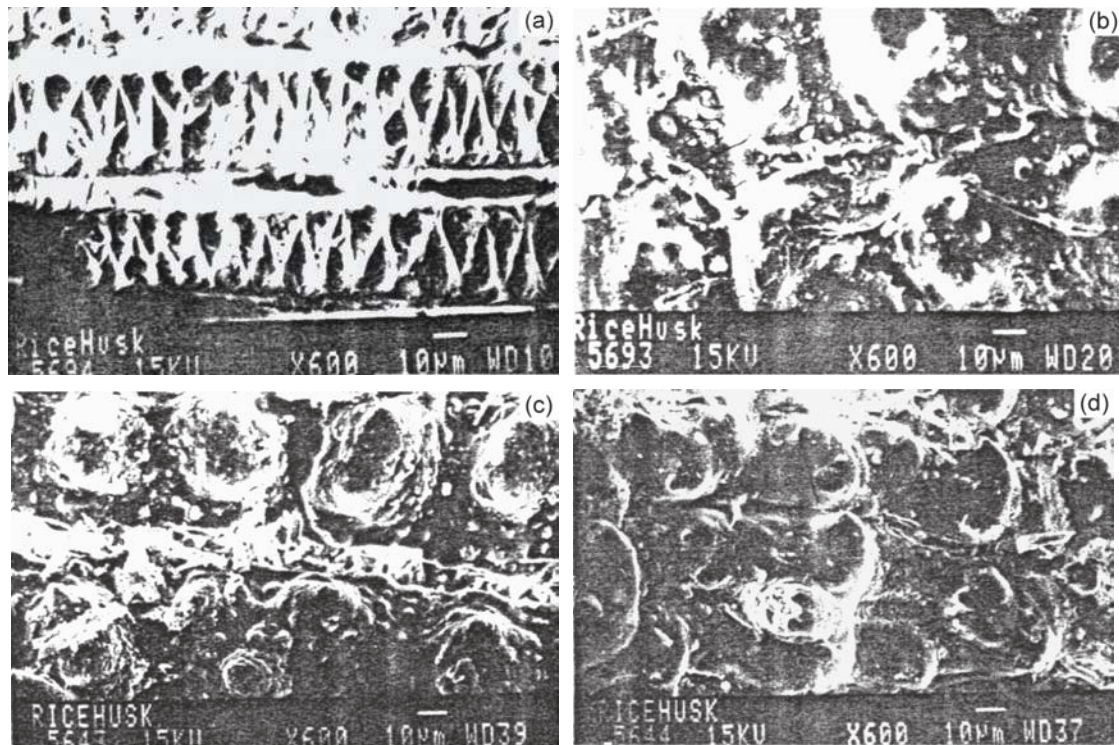
Figure 8: Scanning electron microscopy micrographs of rice husk ash produced in air at (a) 400 °C, (b) 600 °C (c) 750 °C and (d) 900 °C, showing increasing cavitation.
[Figura 8: Micrografias obtidas em microscópio eletrônico de varredura de cinza da palha de arroz produzida ao ar a (a) 400 °C, (b) 600 °C (c), 750 °C and (d) 900 °C.]
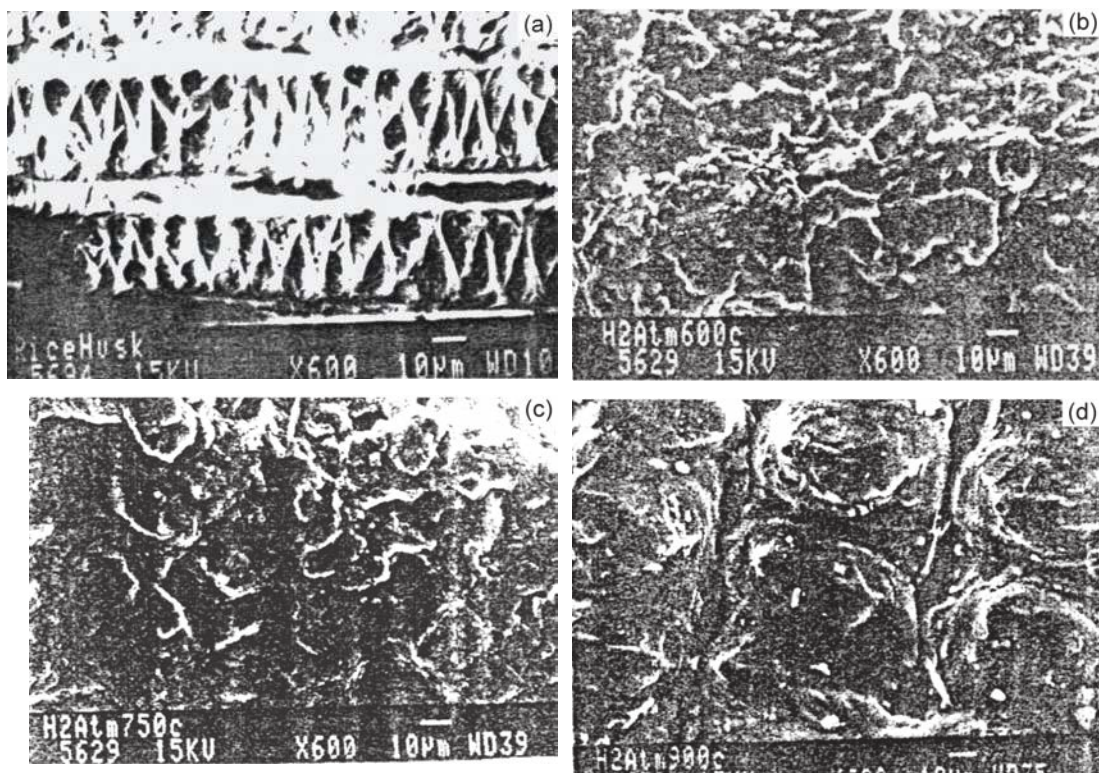

Figure 9: Scanning electron microscopy micrographs of rice husk ash produced in hydrogen at (a) 400 °C, (b) 600 °C (c) 750 °C and (d) 900 °C.
[Figura 9: Micrografias obtidas em microscópio eletrônico de varredura de cinza da palha de arroz produzida sob hidrogênio a (a) 400 °C, (b) 600 °C, (c) 750 °C and (d) 900 °C.]
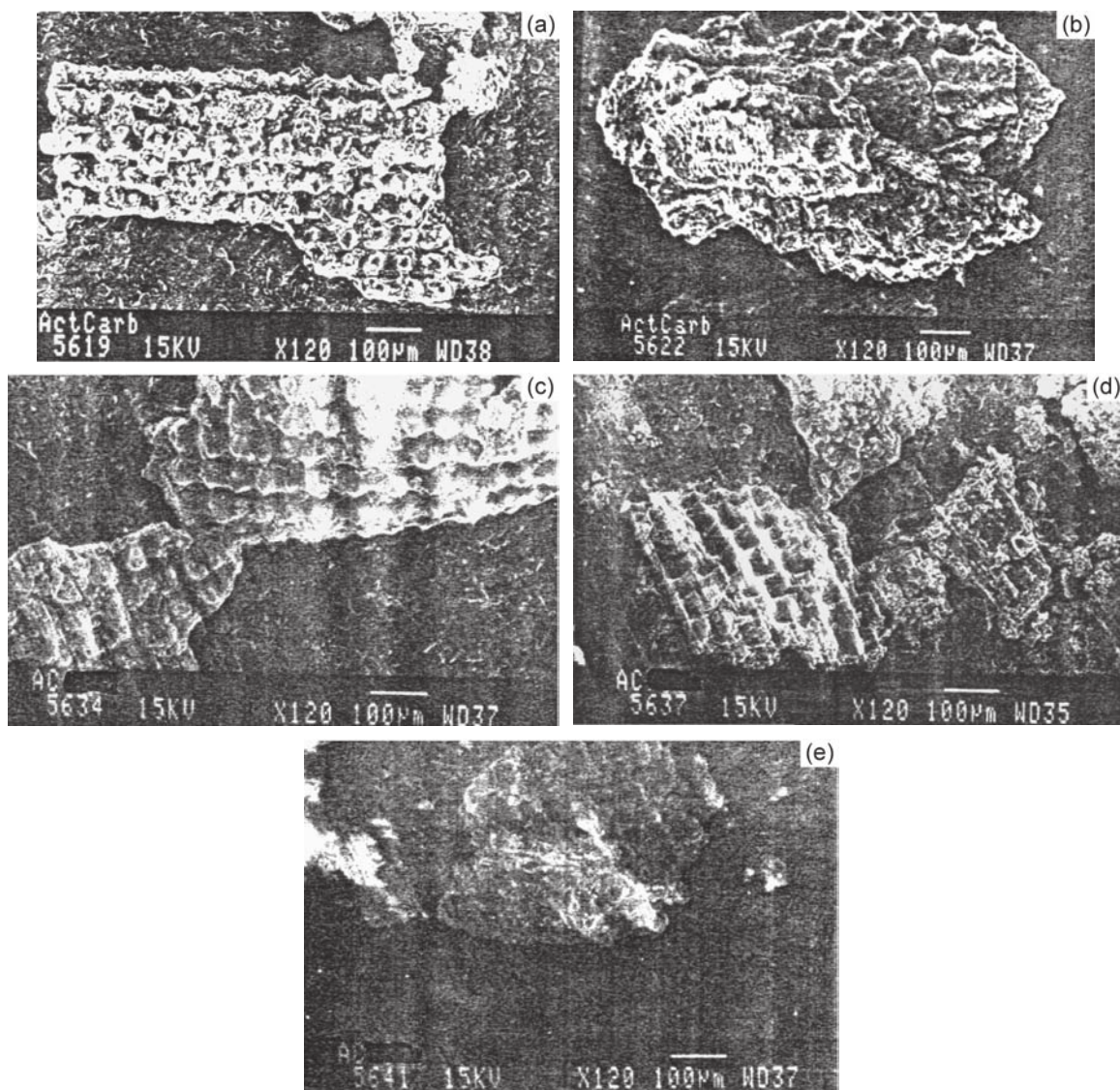
Figure 10: Scanning electron microscopy micrographs of activated husk ash produced at (a) 600 °C, (b) 700 °C, (c) 800 °C, (d) 900 °C and (e) 1000 °C, magnified 120 times.
[Figura 10: Micrografias obtidas em microscópio eletrônico de varredura de cinza da palha de arroz ativada produzida a (a) 600 °C, (b) 700 °C, (c) 800 °C, (d) 900 °C e (e) 1000 °C. Aumento: 120x.]

(silica) passes through maxima with continuously changing slope. Sharp fall in surface area rate at high temperature range (above 1100 K) can be attributed to crystallization due to formation of calcium phosphosilicates revealed by sharp peaks in XRD pattern (Fig. 2).

Morphology of husk flakes shows some what similar changes with firing temperature in air or hydrogen. As shown in Figs. 8 and 9, large cavities become predominant with increasing temperature. However preponderance of cavitation with rising burning temperature is some what less in the case of charring in hydrogen atmosphere. Figs. 10 and 11 show the successive micrograph of phosphoric acid activated rice husk flakes produced at different temperature. The micrograph corresponding to high temperature (800 °C and 900 °C) show cavitation collapse. This may be attributed to

solid state reaction between phosphoric acid and silica leading to formation of calcium phosphosilicate as evident in sharp XRD peaks (Fig. 2). Husk burning charring temperature has effect on chemical composition also due to sublimation of some components during processes. This is shown in Fig. 11. These indicate that non silica components also come out of ash along with stream of hydrocarbon vapour possibly.

Mainly elements silicon, potassium, calcium and iron were considered. The variation of weight percent of these elements in samples produced at different temperatures is shown in Figs. 12a and 12b, which shows continuously increasing concentration of silicon, in contrast to decreasing trend of remaining three elements. It seems that potassium, calcium and iron are present in some form of hydrated salts which sublimates with increasing process temperature.
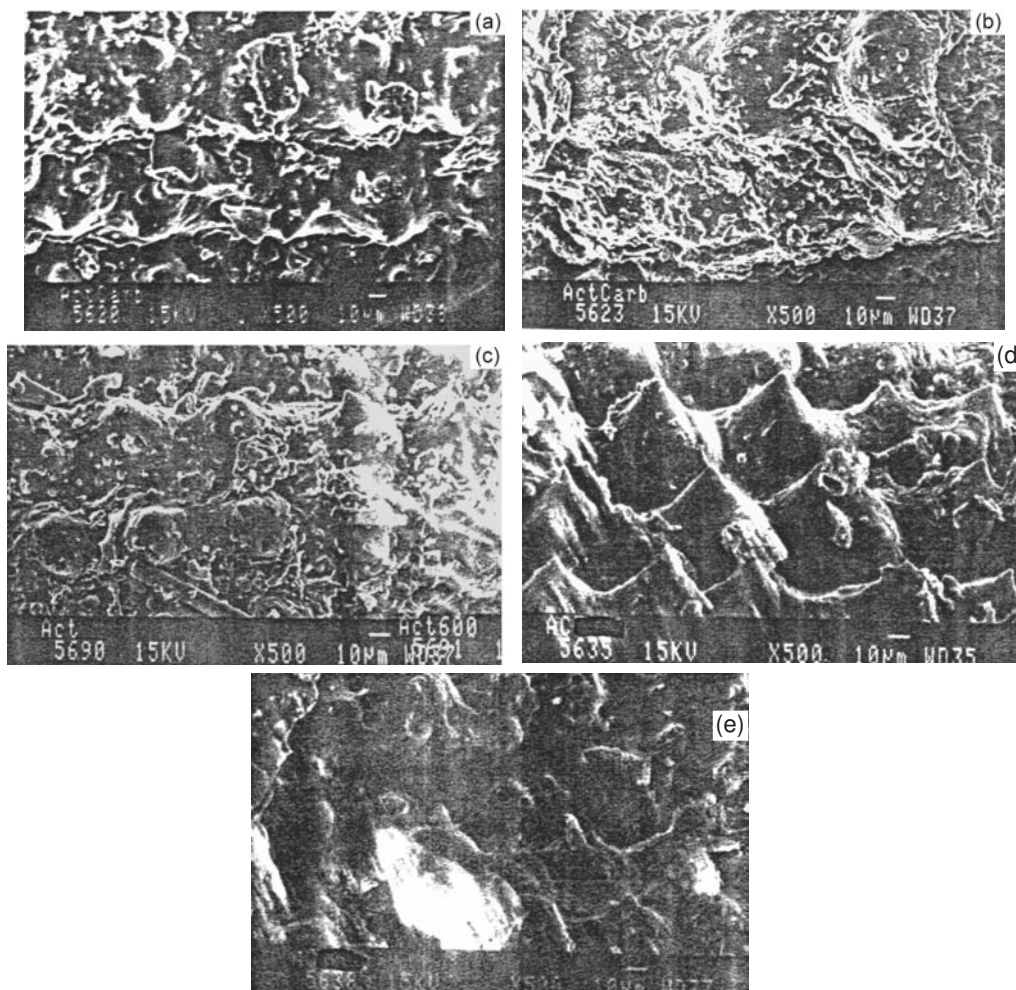
Figure 11: Scanning electron microscopy micrographs of activated husk ash produced at (a) 600 °C, (b) 700 °C, (c) 800 °C, (d) 900 °C and (e) 1000 °C, magnified 500 times.
[Figura 11: Micrografias obtidas em microscópio eletrônico de varredura de cinza da palha de arroz ativada produzida a (a) 600 °C, (b) 700 °C, (c) 800 °C, (d) 900 °C e (e) 1000 °C. Aumento: 500x.]
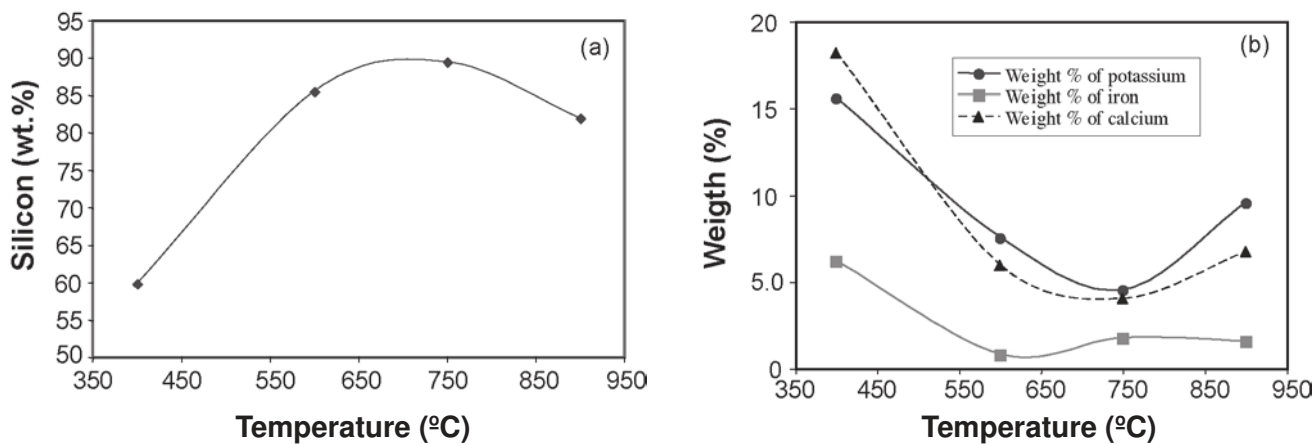

Figure 12: Variation of weight percent of (a) silicon (b) potassium, calcium and iron with temperature in rice husk ash produced in air.
[Figura 12: Variação dos teores de silício (a), potássio, cálcio e ferro (b) com a temperatura na cinza da palha de arroz produzida ao ar.]

Especially potassium oxide is known to sublimate slowly with increasing temperature. It may be that potassium, calcium and iron all are in some complex form, which on increasing process temperature comes out of the silica matrix
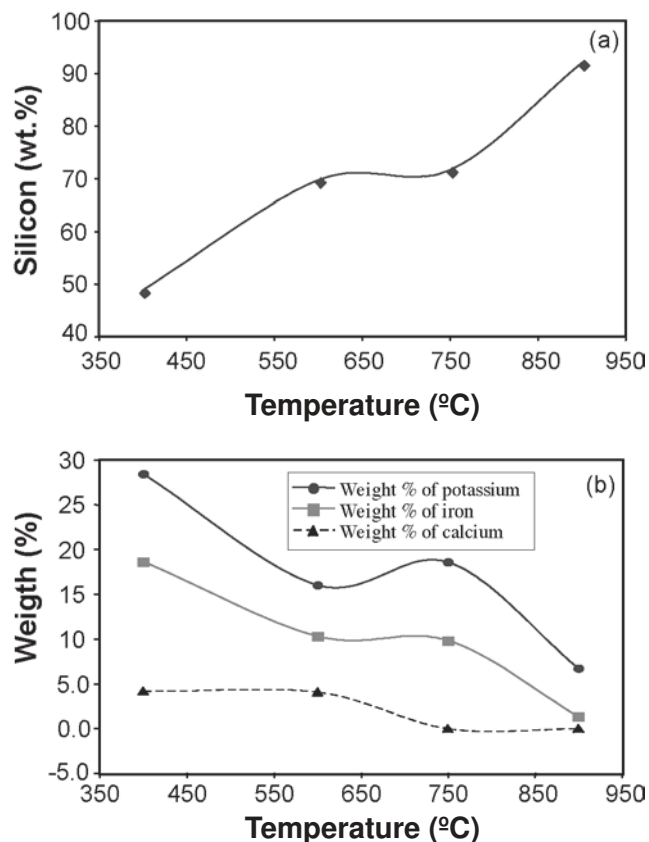
Figure 13: Variation of weight percent of (a) silicon (b) potassium, calcium and iron with temperature in rice husk ash produced in hydrogen.
[Figura 13 : Variação do teor de silício (a) e potássio, cálcio e ferro (b) com a tempertaura em cinza da palha de arroz produzida sob hidrogênio.]

Figure 14: Variation of percent decolorization of (a) molasses solution (b) iodine solution with amount of samples.
[Figura 14: Variação percentual da descolorização de (a) solução de melaço e (b) solução de iodo com o teor de amostras.]

leading to apparent enhancement of silicon. The samples prepared in hydrogen atmosphere were also analyzed for the presence of silicon, potassium, calcium and iron. It is evident from the Fig. 13a that the relative weight percent of silicon increases, while that of other three elements (Fig. 13b) decreases. It seems that potassium, calcium and iron are present in some oxide form or as hydrated salts, which sublimates at increasing process temperature. It may be that potassium, calcium and iron all are in some complex form or forms complex under process condition, which on increasing process temperature comes out of the silica matrix leading to apparent enhancement of silicon percent.

The results of molasses test as prescribed by [28] for decolorization were obtained for all the three kinds of material prepared. The variation of percent decolorization of molasses solution with the amount of samples, for all the three materials are shown in Fig. 14a. It is evident that percent decolorization of molasses solution increases with the amount of ash used in all the cases. The variation is linear for the samples prepared in air and hydrogen. However, the activated husk sample shows mild curvature towards decolorization axis showing better efficiency with increasing
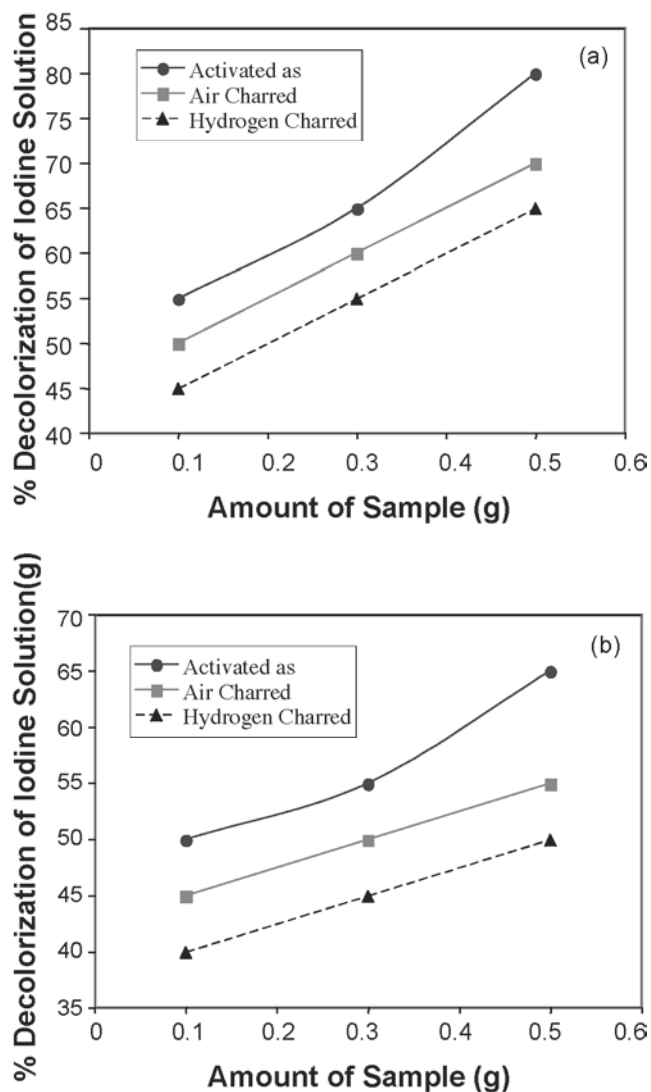
amount. Slope of the lines (curves) in all the three cases are nearly same indicating identical adsorption mechanism. The decolorization curves for different materials lie one over another. This indicates that activated husk has maximum activity and hydrogen charred husk has minimum activity.

The iodine decolorization tests for all the three type of materials are shown in Fig. 14b. Decolorization in the present case is quite similar to that of molasses test. However, percent activity in this case is certainly smaller in comparison to molasses test.

CONCLUSIONS

Air burnt, hydrogen charred and activated rice husk ash has been prepared and characterized for their surface area stability with temperature, BET particle size and

decolorization activity of molasses/iodine solution. The maximum surface area observed is ~180 m^2/g for air burnt ash, 118 m^2/g for hydrogen charred ash and 112 m^2/g for activated ash. While surface area decreases with temperature for air burnt ash, it increases with temperature for air hydrogen charred ash. The activation barrier for densification (surface area reduction) with temperature is due to surface diffusion at low temperature and due to bulk diffusion at high temperature ranges. The particle size variation with temperature for air burnt ash is between 6 to 84 nm and for hydrogen charred ash is between 190 nm to 10 nm. Decolorization activity is maximum for activated air burnt ash and minimum for air charred ash.

ACKNOWLEDGEMENTS

REFERENCES

[1] P. K. Basu, S. K. Roy, J. Das, A. Bhattacharjee, S. K. Roy. (Indian IN 168,399 (C1 B01J 29/04), 23 March 1991, Appl. 87/DE990 (18 Nov. 1987) 15 pp.

[2] M. Tomozawa, D. L. Kim, V. Lou, Preparation of high purity, low water content fused silica glass, J. Non-Cryst. Solids **296** (2001) 102-106.

[3] P. A. Tanner, B. Yan. H. Zhang, Preparation and luminescence properties of sol-gel hybrid materials incorporated with europium complexes, J. Mater. Sci. **35** (2000) 4325-4328.

[4] G. Wu, J. Wang, J. Shen, T. Yang, Q. Zhang, B. Zhou, Z. Deng, F. Bin, D. Zhou, F. Zhang. Properties of sol–gel derived scratch-resistant nano-porous silica films by a mixed atmosphere treatment, J. Non-Cryst. Solids **275** (2000)169-174.

[5] Y. Xu, S. Wang, Z. Qiu, Faming Zhaunli Shenqing Gongkai Shuomingshu CN. 1,111,213 (C1 C01B 31/36), 8 Nov 1995, Appl. 94,114,319 (30 Dec. 1994) 7 pp.

[6] A. S. Vlasov, A. I. Zakharov, O. A. Sakisyan, N. A. Lukasheva, Ogneupory **10** (1991) 15-17 (in Russian).

[7] J. M. Chen, W. Feg, Phys. Sci. Eng. **15,** 5 (1991) 412-50.

[8] N. Ikram, M. Akhter, J. Mater. Sci. **23**, 7 (1988) 2379-81.

[9] M. Nakagawa, Kogyo Zairo **45**, 7 (1997) 82-88.

[10] K. C. Nandi, D. Mukherjee, A. K. Biswas, H. N. Acharya, J. Mater. Sci. Lett. **12**. 16 (1993) 1248-50.

[11] J. Yu, G. Xu, G. Zhao, S. Shan, Guisuanyan Tonghao 15, 3 (1996) 48-51.

[12] Z. Liu, Faming Zhuanli Shenqing Gongkai Shuomingshu CN, 1,090,306 (C1.C09C 1/28), 03 Aug. 1994, Appl. 93,103,043 (20 March 1993) 11 pp.

[13] M. Patel, A. Karere, P. Prasanna, Effect of thermal and chemical treatments on carbon and silica contents in rice husk, J. Mater. Sci**.** **22** (1987) 2457-2464.

[14] H. Hayasi, S. Nakashima, Synthesis of trioctahedral smectite from rice husk ash as agro-waste, Clay Sci. **8**, 4 (1992) 181-193.

[15] C. B. Cook, P. R. S. Speare, J. B. Tebbit, (Kingsway Group PLC) PCT Int. Appl. WO 95,10,488 (C1 C04B 18/10), 20 Apr. 1995, GB Appl. 93/21, 359 (15 October 1993) 22 pp.

[16] A. Chakraverty, S. Kaleemullah, Conversion of rice husk into amorphous silica and combustible gas: Energy Conversion and Managem. **32,** 6 (1991)565-570.

[17] X Huang, Faming Zhuanli Shenging Gongkai Shuomingshu CN 86,104,705 (C1. C01B 33/133) (18 May 1988) p. 8.

[18] G. M. Rao, A. R. K. Sastry, P. K. Rohatgi, Mater. Sci. Bull. **12** (1989) 469-479.

[19] T. B. Ghosh, K. C. Nandi, H. N. Acharya, D. Mukherjee, Mater. Lett. **12,** 3 (1991) 175-178.

[20] J. P. Communal, F. Fabre, Y. Mottot, Eau, Ind. Nuisances **192** (1996) 35-38.

[21] M. Fukazawa, (Tokai Carbon Kk) Jpn. Kokai Tokkyo Koho Jp 07,149,921 [95,149,921] (C1. C08J 5/14) (13 June 1995) pp. 6.

[22] U. Kalapathy, A. Proctor, J. Shultz, An improved method for production of silica from rice hull ash, Bioresour. Techn. **85** (2002)285-289.

[23] N. Yalcin, V. Sevinc, Studies on silica obtained from rice husk, Ceram. Int. **2**, 2 (2001) 219-224.

[24] V. P. Della, I. Kuhn, D. Hotza, Rice husk ash as an alternate source for active silica production, Mater. Lett. **57** (2002) 818-821.

[25] L. Tzong-Horng, Preparation and characterization of nano-structured silica from rice husk, Mater. Sci. Eng. A **364** (2004) 313-323.

[26] Z. Jiang, R. A. Brown, MRS Proc., Defect and Impurity Engineered Semiconductor Devices (1995).

[27] K. Keunyoo, H. L. Young, H. Myung, Semicond. Sci. Technol. **11** (1996) 1059-1064.

[28] J. W. Hasler, Purification with activated carbon, Chemical Publ. Co., New York, USA (1974).